

A fiber bundle structure with uniform transmission characteristics for high-density astronomical optical cables

Qi Yan¹, Tao Geng¹, Hang Jiang¹, Chuang Zhao¹, Ying-Hua Zhang¹, An-Zhi Wang¹, Jia-Bin Wang¹, Xi-Ren Jin¹, Xu-Dong Chen¹, Chun-Lian Lu¹, Liang Wang², Zhi-Xin Huang², Jing-Dong Zhuang², Song Wang², Wei-Min Sun^{1*} and Xiang-Qun Cui³

¹ Key Lab of In-fiber Integrated Optics, Ministry Education of China, Harbin Engineering University, Harbin 150001, China; sunweimin@hrbeu.edu.cn

² Yangtze Optical Fibre and Cable Joint Stock Limited Company, Wuhan 430073, China

³ Nanjing Institute of Astronomical Optics and Technology, National Astronomical Observatories, Chinese Academy of Sciences, Nanjing 210042, China

Received 2019 January 8; accepted 2019 April 3

Abstract Transmission efficiency (TE) and focal ratio degradation (FRD) are two important parameters for evaluating the quality of an optical fiber system used for astronomy. Compared to TE, the focal ratio is more easily influenced by external factors, such as bending or stress. Optical cables are widely implemented for multi-object telescopes and integral field units (IFUs). The design and fabrication process of traditional optical cables seldom considers the requirements of astronomical applications. In this paper, we describe a fiber bundle structure as the basic unit for miniaturized high-density FASOT-IFU optical cables, instead of the micro-tube structure in stranded cables. Seven fibers with hexagonal arrangement were accurately positioned by ultraviolet (UV)-curing acrylate to form the bundle. The coating diameter of a fiber is 0.125 mm, and the outer diameter of the bundle is 0.58 mm. Compared with the 0.8 mm micro-tube structure of a traditional stranded cable, the outer diameter of the fiber bundle was reduced by 27.5%. Fiber paste was filled into the bundle to reduce stress between the fibers. We tested the output focal ratio (OFR) in 95% of the encircled energy (EE95) of the fibers in the bundle under different conditions. With the incident focal ratio $F/8$, the maximum difference of OFR is 0.6. In particular, when the incident focal ratio is $F/5$, the maximum difference of OFR is only 0.1. The jacket formed by the UV-curing acrylate can withstand a certain stress of less than 1.38 N mm^{-1} . The fiber bundle can maintain uniform emitting characteristics with a bending radius of 7.5 cm and with tension less than 6 N. The test results show that the structure of the fiber bundle can be used as a basic unit for miniaturized high-density astronomical optical cables.

Key words: instrumentation: spectrographs — techniques: imaging spectroscopy — techniques: spectroscopic — methods: miscellaneous

1 INTRODUCTION

As an important medium for collecting and transmitting light, optical fibers are now widely utilized in astronomical spectrographs. In recent years, the number of optical fibers applied to multi-object spectrographs and integral field unit (IFU) technology has been increasing. LAMOST with 4000 fibers (Cui et al. 2012), DESI with 5000 fibers (Flaughner & Bebek 2014), VIRUS for HET with 32 604 fibers (Hill et al. 2004; Lee et al. 2010; Hill

et al. 2014; Kelz et al. 2014; Vattiat et al. 2016), and DOTIFS for the 3.6 m DOT with 2304 fibers (Chung et al. 2014; Chattopadhyay et al. 2018; Chung et al. 2018) have been reported. Astronomical spectrographs require the optical fiber system to have optimal optical behaviors. Transmission efficiency (TE) and focal ratio degradation (FRD) are the two important parameters for evaluating the quality of an optical fiber system (Murphy & Hill 2012).

Enclosing the fibers in a cable is an effective way to protect optical fibers from outside mechanical forces and water vapor, and improve the reliability and service life

* Corresponding author

of the observation equipment. This is also beneficial for wiring and maintenance of the fibers. Fiber optic cables are widely used in modern communication networks, and their structure is constantly updated to meet the needs of different types of communication. Sumitomo Electric Industries fabricated an ultra-high-fiber-count and high-density optical cable with 3456 fibers and an outer diameter of 34 mm (Sato et al. 2017). In the process of fabricating a fiber optical cable, stress between the optical fibers will be introduced. The design of a cable with the traditional structure only considers the TE of the cable, but regards the FRD less. Previous studies have confirmed that stress is a fundamental cause of FRD. Murray et al. (2017) of Durham University proposed an optimal method for producing low-stress fiber optic cables for astronomy and suggested fill factors lower than 50%.

We will manufacture an IFU with $64 \times 63 \times 2$ fiber elements for the second generation Fiber Arrayed Solar Optical Telescope (FASOT) (Qu. 2011; Qu et al. 2014; Zhi et al. 2016), named FASOT-2, which has a 600 mm $F/12$ Gregorian telescope. By using polarimetric optic switching (POS) and the IFU, FASOT will achieve real-time, high-efficiency and high-precision spectropolarimetry of multiple magneto-sensitive lines over a two-dimensional field of view. The first challenge is the production of the fiber optic cables. In order to improve the precision of polarization measurement, fibers in the IFU should have uniform and stable transmission characteristics when the telescope is operating. Also, the cable should be miniaturized, high-density and soft, to reduce the weight of the IFU, which influences the tracking accuracy of the telescope. The traditional stranded cable, which employs a micro-tube as the basic unit, requires low fill factors to keep a low FRD of the fibers in the cable. It is a disadvantage to the design of miniaturized, high-density, soft optical cables. In collaboration with the Yangtze Optical Fibre and Cable Joint Stock Limited Company (YOFC), we designed and manufactured the optical cable for FASOT-IFU. A fiber bundle structure was designed and manufactured to be the basic unit for the miniaturized, high-density FASOT-IFU optical cables. In this paper, we compared the static test results of the fiber bundle structure with the micro-tube structure. We also dynamically test the transmission characteristics of the fiber bundle under different bending radius, tension and pressure conditions.

2 THE STATE OF OPTICAL FIBERS IN AN OPTICAL CABLE

The fibers in a tube form the basic unit of a traditional stranded fiber cable used for communication. The tubes wind spirally around the center of the cable without imparting a twist to the tubes. The first criterion of the fibers

in the cable is no tension when the cable is bent or pulled (Murray et al. 2017), so that the basic unit around the core is longer than the cable in order to keep the fibers in a relaxed state. This is called the fiber excess length. The model of the fibers in the cable can be described as a helix, as illustrated in Figure 1(a), and the equation describing the track of a fiber is

$$r = tx + R \sin\left(\frac{2\pi t}{P}\right)\mathbf{y} + R \cos\left(\frac{2\pi t}{P}\right)\mathbf{z}, \quad (1)$$

where R is the distance between the center of the fiber and the center of the cable, P is the stranding pitch of the cable, t is a parametric variable, from 0 to P , and \mathbf{x} , \mathbf{y} and \mathbf{z} are directional basis vectors.

The length of fiber L_f in one period, as delineated by the black line in Figure 1(b), is

$$L_f = \sqrt{(2\pi R)^2 + P^2}. \quad (2)$$

The fiber excess length ε is

$$\varepsilon = \frac{L_f - P}{P}. \quad (3)$$

The cable length changes with environmental temperature or when external force is applied on the cable, whereas the length of the fiber remains the same. There are two different conditions for the cable, i.e., stretched and compressed. Both of the two conditions will change the relative position of the fibers and the tube, and will also change the relative position of the tubes and the cable. When the cable length is stretched, the fibers move to the center of the optical cable, as shown in Figure 2. Also, when the cable becomes too long, the fibers will break. If the distance between the center of a fiber and the center of the cable reduces by ΔR , and the stranding pitch of the cable P increases by ΔP , as illustrated by the blue line in Figure 1(b), the length of fiber L_f becomes

$$L_f = \sqrt{[2\pi(R - \Delta R)]^2 + (P + \Delta P)^2}. \quad (4)$$

As depicted in Figure 3, when the cable is compressed, the fibers move to the outer ring of the cable; when the cable becomes too short, the fibers would experience loss from microbending. When the distance between the center of a fiber and the center of the cable increases by ΔR , the stranding pitch of the cable P reduces by ΔP , as traced by the red line in Figure 1(b), and the length of fiber L_f is

$$L_f = \sqrt{[2\pi(R + \Delta R)]^2 + (P - \Delta P)^2}. \quad (5)$$

Fibers in the tube are squeezed by other fibers or by the wall of the tube around it. Tubes in the cable are squeezed by other tubes, or by the jacket of the cable. A change in the position of an optical fiber in the cable means a change of stress on the optical fiber. The fill factor η of fibers in

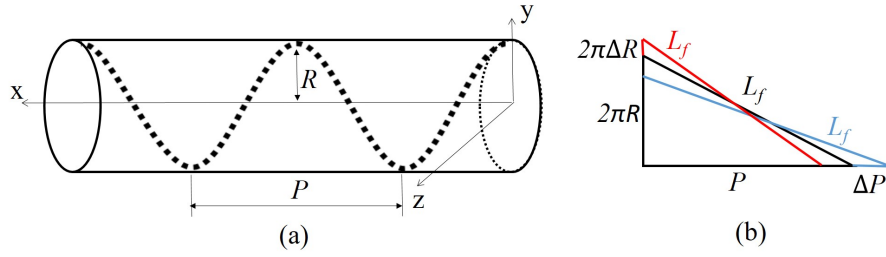


Fig.1 The model of a fiber in the tube can be described as a helix.

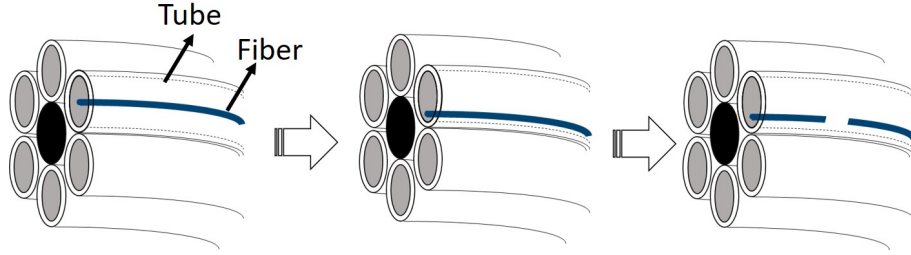


Fig.2 Schematic diagram of fiber state during the process of stretching an optical cable.

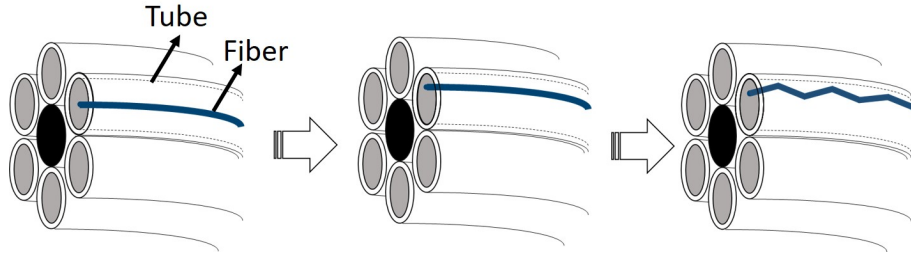


Fig.3 Schematic diagram of fiber state during the process of compressing an optical cable.

the tube can be used to characterize the stress on fibers in a tube. It is the ratio of the equivalent area of the fiber bundle A_{fibers} to the cross-sectional area of the bore of the tube A_{tube} , and can be expressed as

$$\eta = \frac{A_{\text{fibers}}}{A_{\text{tube}}} = \frac{\pi R_{\text{fiber}}^2}{\pi R_{\text{IRT}}^2}, \quad (6)$$

where R_{IRT} is the inertial radius of the tube, and R_{fiber} is the equivalent radius of the fiber bundle. When the number of fibers in a tube $N \leq 7$, the arrangement of fibers is as depicted in Figure 4. Also R_{fiber} is

$$\begin{cases} R_{\text{fiber}} = r + \frac{r}{\sin \alpha}, \\ \alpha = \frac{\pi}{N}, \quad (N \leq 7) \end{cases} \quad (7)$$

where r is the radius of a fiber.

When the number of fibers in a tube $N > 7$, the equivalent radius R_{fiber} can be described as the radius of N fibers in a hexagonal close-packed array (Cheng, 2016)

$$R_{\text{fiber}} = 1.16\sqrt{N} \times r. \quad (N > 7) \quad (8)$$

The larger the fill factor is, the more strongly the fibers are bound, which means the stress on the fibers in the tube

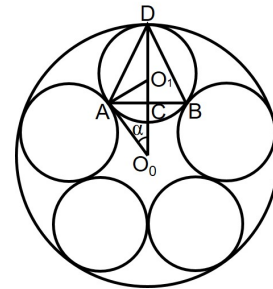


Fig.4 Arrangement of fibers in a tube when $N \leq 7$.

is greater. For the different fibers in the tube with different positions and state, the effect of stress on different fibers is non-uniform, which leads to differences in the FRD. When the cable state changes, the stress on the fibers changes, and the FRD also changes.

3 THE RAPID TEST PLATFORM FOR ASTRONOMICAL FIBER FOCAL RATIO

The IFU for FASOT would use 8064 fibers to receive optical information from the Sun. It would be a large, time-

Table 1 The Stranded Cable Parameters

Number of fibers in the cable	704
Number of micro-tubes	88
Number of fibers in a micro-tube	8
Fiber outer diameter (mm)	0.125
Fiber core diameter (mm)	0.035
Unit weight (kg m^{-1})	0.104
Inner diameter of the inner sheath (mm)	10
Outer diameter of cable (mm)	13.5
Inner diameter of the micro-tube (mm)	0.5
Outer diameter of the micro-tube (mm)	0.8
Minimum bending radius (m)	<0.45

Table 2 Testing Results for an 18 m Stranded Cable with Incident Focal Ratio F/8

Fiber number	State 1		State 2		State 3	
	OFR	TE	OFR	TE	OFR	TE
1	6.4	87.8%	6.5	86.6%	4.6	86.5%
2	5.6	88.6%	7.1	86.5%	5.0	87.8%
3	4.3	87.3%	6.5	86.8%	5.4	86.7%
4	5.9	86.8%	6.5	86.8%	5.2	86.7%
5	5.0	87.5%	6.7	86.2%	4.7	86.8%
6	5.1	87.4%	5.9	86.9%	4.6	87.8%
7	5.6	87.4%	6.0	86.6%	5.3	87.1%
8	5.4	87.5%	6.3	86.7%	5.0	87.1%
Average	5.4	87.5%	6.3	86.7%	5.0	87.1%
Maximum difference	2.1	1.8%	1.6	0.9%	0.8	1.1%

Table 3 The Main Parameters of the Fiber Bundle

Number of fibers in a bundle	7
Fiber outer diameter (mm)	0.125
Fiber core diameter (mm)	0.035
Outer diameter of bundle (mm)	0.580

Table 4 Testing Results for a 10 m Fiber Bundle with Different Incident Focal Ratios

IFR	F/8		F/7		F/6		F/5	
	OFR	TE	OFR	TE	OFR	TE	OFR	TE
1	6.0	87.1%	5.7	87.3%	5.4	87.3%	4.7	87.2%
2	5.6	87.2%	5.3	87.3%	5.0	87.4%	4.7	86.3%
3	5.6	87.1%	5.1	87.5%	4.9	87.5%	4.6	87.1%
4	6.0	87.4%	5.4	87.7%	5.2	87.4%	4.7	87.9%
5	6.2	87.2%	5.6	87.6%	5.2	87.7%	4.7	88.1%
6	5.7	87.4%	5.6	87.5%	5.1	87.7%	4.7	87.2%
7	6.2	87.0%	5.6	87.5%	4.8	87.5%	4.6	86.5%
Average	5.9	87.2%	5.5	87.5%	5.1	87.5%	4.7	87.2%
Maximum difference	0.6	0.4%	0.6	0.4%	0.6	0.4%	0.1	1.8%

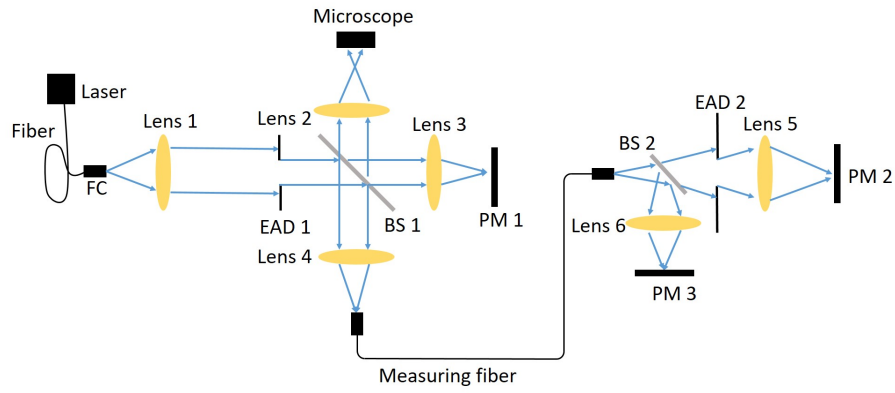


Fig. 5 Schematic diagram of the rapid test platform for an astronomical fiber.

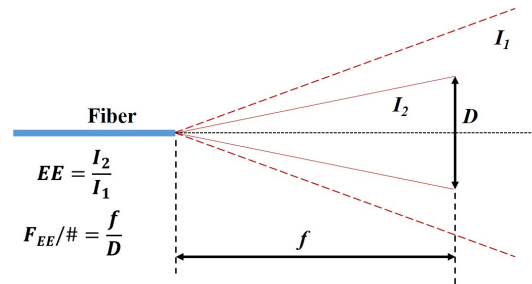


Fig. 6 EE characterizes the percentage of energy in the measured focal ratio to total energy.

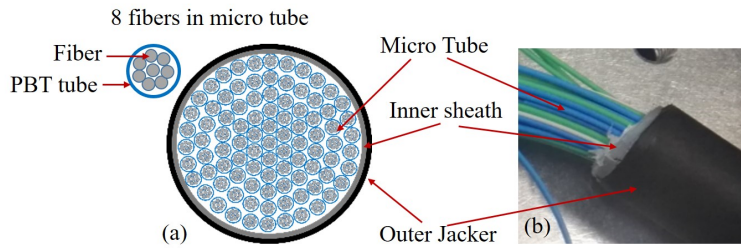


Fig. 7 A stranded cable with 704 fibers.

consuming task to test the transmission characteristics of the fibers and IFU. Here, we employed a rapid test platform to test the TE, output focal ratio (OFR) in a certain encircled energy (EE) and fiber surface quality simultaneously. In addition, this modified platform can compensate the energy fluctuation of the light source. A schematic diagram of the platform is shown in Figure 5. Details about the measurement methods and theories were described by Yan et al. (2018). As illustrated in Figure 6, EE characterizes the percentage of energy in the measured focal ratio to total energy. We tested the OFR of 95% of the encircled energy (EE95). The test results include the error caused by polishing the end surface and the error from incident light.

4 TRADITIONAL MINIATURIZED STRANDED OPTICAL FIBER CABLE.

For the FASOT-IFU, we made a model of an 18 m cable for testing. This model had the structure of a traditional miniaturized stranded fiber optic cable with 704 fibers as illustrated in Figure 7. The cable had 88 micro-tubes, and each tube contained eight fibers within it. The micro-tubes were made of polybutylene terephthalate (PBT) with an inner diameter of 0.5 mm and an outer diameter of 0.8 mm; the detailed parameters are shown in Table 1. To reduce costs, there was one tube with eight useful fibers, and others were discarded. We tested the transmission characteristics of fibers in the cable with the incident focal ratio $F/8$ and in three different cases. For case one, we used tape to fix the cable on the floor to simulate the actual optical fiber cable wiring. For case two, the cable was in a relaxed state

on the floor. For case three, we measured the cable at the minimum bending radius of 0.45 m. The testing results are provided in Table 2 and Figure 8. The OFR of each fiber in the tube is quite different. The stress from the tape would reduce the average of the OFR, and at the same time increase the difference between different fibers. Due to the high stress, bending would reduce the average of the OFR, and increase the uniformity of the OFR.

The main factor causing non-uniform OFR is the non-uniform stress on the fibers. The fill factor of this tube with eight fibers is 67.2%. The larger fill factor causes serious stress on the fibers in the cable. When the cable state changes, the OFR also changes. It can be noted that local stress on the cable leads to a large difference in OFR. The bending of the optical cable causes an increase in FRD, but a decrease in the difference of the OFR. The thin and soft PBT shell of a tube cannot stop the stress from other tubes or the jacket of the cable, which is another factor causing non-uniform stress on the fibers. A thicker and harder shell is needed. However, low fill factors and a thick shell of the tube would increase the size and weight of the cable. These are adverse conditions for the design of the miniaturized, high-density, soft cable for FASOT-IFU. We present a fiber bundle structure with uniform transmission characteristics as the basic unit of the cable for FASOT-IFU, which is conducive to miniaturized, high-density optical cables in astronomy.

5 FIBER BUNDLE WITH UNIFORM AND STABLE TRANSMISSION CHARACTERISTICS

As learned from experience gained in the manufacturing process of a fiber ribbon used in optical devices, we made a fiber bundle with uniform and stable transmission characteristics to be the basic unit for the miniaturized, high-density FASOT-IFU optical cables.

5.1 The Structure of the Fiber Bundle

Fibers in a tube with uniform transmission characteristics require the fibers to be subjected to uniform stress. Stable transmission characteristics require that the fibers should stay stable even if the cable state changes. For this reason, we designed and fabricated a fiber bundle structure instead of the micro-tube structure in the stranded cable, as shown in Figure 9. Table 3 lists the main parameters of the proposed fiber bundle structure. Compared with the micro-tube structure, the outer diameter of the bundle structure reduced 27.5%. The fibers were accurately positioned and then encapsulated by the UV-curing acrylate to form a bundle. The fiber paste was filled into the bundle to reduce the friction between fibers. Seven fibers with a hexagonal arrangement have a stable structure. As a whole, fibers in

the bundle keep their positions and maintain the same state when the bundle's state changes. The jacket outside the fiber bundle formed by the acrylate can withstand a certain amount of external stress. The UV-curing acrylate should have low stress and separate from optical fibers easily after curing. As shown in Figure 10, with the incident focal ratio $F/8$ and the relaxed state, the fiber bundle has a more uniform OFR than the stranded cable with the micro-tube. The length of the tested bundle is 20 m, 2 m longer than the model cable, so that the TE is lower. This structure of the fiber bundle is more compact and has uniform transmission characteristics, which can form the basic unit for miniaturized high-density optical cables. We tested the transmission characteristics of optical fibers under different conditions.

5.2 The FRD with Different Incident Ratios

Firstly, we measured the transmission characteristics of a 10 m fiber bundle in the relaxed state with different incident focal ratios. The result is shown in Table 4 and plotted in Figure 11. Figure 11(a) and 11(b) are the OFR and TE with different incident focal ratios, respectively. For the incident focal ratio $F/8$, $F/7$ and $F/6$, the maximum difference in OFR is 0.6. For the incident focal ratio $F/5$, the maximum difference in OFR is 0.1. The fiber bundle has a more uniform OFR with the incident focal ratio $F/5$.

5.3 The FRD with Different Lengths

We measured the transmission characteristics of the fiber bundle with different lengths (10 m, 20 m and 30 m) in the relaxed state when the incident focal ratio is $F/8$. The results are shown in Table 5 and plotted in Figure 12. Figure 12(a) and Figure 12(b) are the OFR and TE of the fiber bundle with different lengths, respectively. The increase in the length of the fiber bundle leads to the decrease of OFR and TE, but it did not change the uniformity of the output characteristics.

5.4 FRD with Different Bending Radii

The bending characteristic of a fiber bundle is a very important parameter for optical cable design and wiring. We should keep the bending radius of the fiber bundle larger than the designed minimum bending radius. As shown in Figure 13, after 1 m from the exit end of the optical fiber bundle, the fiber bundle was wound on cylinders with fixed diameters. The results are shown in Table 6 and plotted in Figure 14. Changing the bending radius of the fiber bundle will change the state of fibers in the bundle. When the bending radius is 5 cm, which is about 170 times the radius of the fiber bundle, the uniformity of the OFR of the fiber

Table 5 Testing Results for a Fiber Bundle with Different Lengths and Incident Focal Ratio $F/8$

Fiber length	10 m		20 m		30 m	
Fiber number	OFR	TE	OFR	TE	OFR	TE
1	6.0	87.1%	5.3	86.4%	5.3	82.9%
2	5.6	87.2%	5.4	85.3%	5.5	83.3%
3	5.6	87.1%	5.7	86.5%	5.3	83.0%
4	6.0	87.4%	5.3	84.7%	5.5	83.5%
5	6.2	87.2%	5.5	85.1%	5.0	83.5%
6	5.7	87.4%	5.2	85.3%	5.6	83.2%
7	6.2	87.0%	5.3	86.5%	5.5	84.0%
Average	5.9	87.2%	5.4	85.7%	5.4	83.3%
Maximum difference	0.6	0.4%	0.5	1.8%	0.6	1.1%

Table 6 Testing Results for a Fiber Bundle with Different Bending Radii and Incident Focal Ratio $F/8$

Bending radius	No bending		15 cm		12.5 cm		10 cm		7.5 cm		5 cm	
Fiber number	OFR	TE	OFR	TE	OFR	TE	OFR	TE	OFR	TE	OFR	TE
1	6.0	87.1%	6.2	86.7%	6.0	86.8%	6.2	87.1%	6.0	86.9%	6.2	87.0%
2	5.6	87.2%	5.6	87.2%	5.5	87.1%	5.6	87.1%	5.6	87.0%	5.6	87.2%
3	5.6	87.1%	5.7	86.9%	5.5	87.2%	5.6	87.3%	5.5	87.1%	5.3	87.0%
4	6.0	87.4%	5.8	86.6%	6.0	87.2%	6.2	87.3%	6.0	87.2%	6.2	87.2%
5	6.2	87.2%	6.2	86.6%	6.1	86.8%	6.2	87.0%	6.2	86.7%	6.2	86.8%
6	5.7	87.4%	5.8	86.9%	5.8	87.0%	5.7	87.3%	5.6	87.1%	5.8	87.3%
7	6.2	87.0%	6.2	87.0%	5.9	86.6%	6.3	87.1%	6.2	87.0%	6.2	87.1%
Average	5.9	87.2%	5.9	86.9%	5.8	86.9%	6.0	87.2%	5.9	87.0%	5.9	87.1%
Maximum difference	0.6	0.4%	0.6	0.6%	0.6	0.6%	0.7	0.3%	0.7	0.5%	0.9	0.4%

Table 7 OFR of a Fiber Bundle with Tension from 0 N to 7 N and Incident Focal Ratio $F/8$

Fiber number	0N	1N	2N	3N	4N	5N	6N	7N
1	5.8	5.8	5.7	5.8	6.0	5.9	5.9	5.9
2	5.5	5.5	5.5	5.4	5.3	5.4	5.4	4.9
3	6.1	6.1	6.2	6.1	5.9	6.0	5.6	5.5
4	6.0	6.0	5.9	5.9	5.8	5.8	5.5	5.6
5	5.5	5.7	5.6	5.5	5.7	5.5	5.6	5.4
6	6.0	6.1	6.1	5.9	5.9	5.8	6.1	5.5
7	5.9	5.9	6.0	5.8	5.8	5.8	5.7	5.7
Average	5.8	5.9	5.9	5.8	5.8	5.7	5.7	5.5
Maximum difference	0.6	0.6	0.7	0.7	0.7	0.6	0.7	1.0

Table 8 TE of a Fiber Bundle with Tension from 0 N to 7 N and Incident Focal Ratio $F/8$

Fiber number	0N	1N	2N	3N	4N	5N	6N	7N
1	87.6%	87.8%	88.6%	88.9%	88.8%	88.9%	88.7%	88.5%
2	88.3%	88.5%	88.4%	88.5%	88.5%	88.6%	88.7%	88.6%
3	88.4%	87.6%	88.7%	88.6%	88.8%	88.9%	89.2%	89.3%
4	88.0%	87.8%	88.0%	88.2%	87.7%	87.7%	87.9%	87.0%
5	88.0%	88.1%	87.5%	87.7%	87.8%	87.6%	87.7%	87.6%
6	87.7%	87.7%	87.8%	87.8%	87.8%	88.0%	88.3%	88.2%
7	87.6%	87.5%	87.5%	87.4%	87.7%	87.5%	87.5%	86.7%
Average	87.9%	88.0%	88.1%	88.1%	88.2%	88.2%	88.3%	88.0%
Maximum difference	0.8%	1.1%	1.2%	1.5%	1.1%	1.5%	1.6%	2.7%

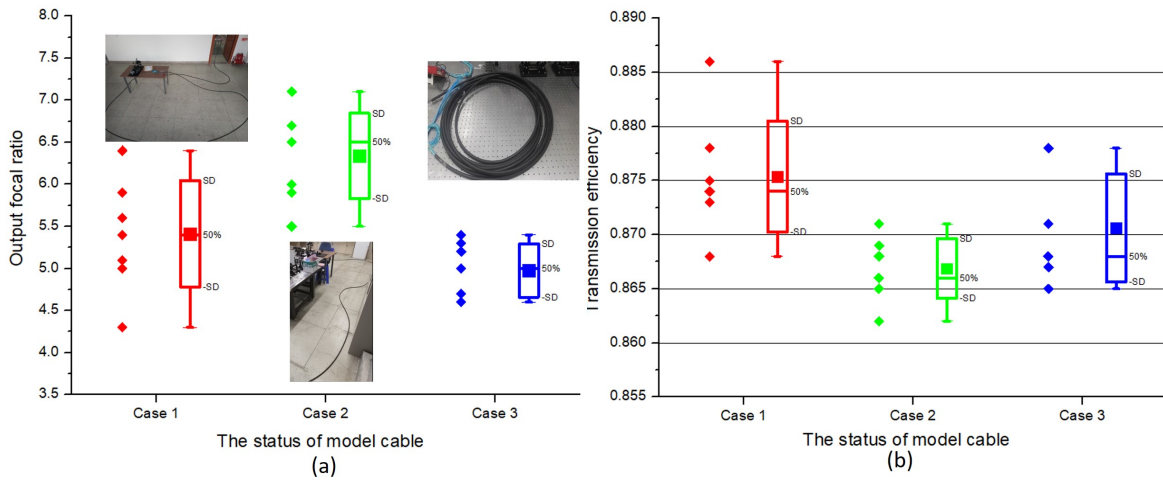


Fig. 8 Transmission characteristics of an 18 m stranded cable with different cases. Case 1: the cable was fixed on the floor with tape; case 2: the cable was in the relaxed state on the floor; case 3: the cable was in the bending state with a minimum bending radius of 0.45 m. (a) Output focal ratio; (b) TE.

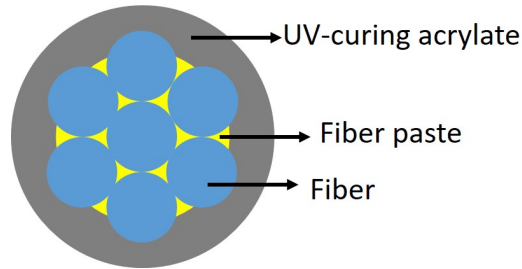


Fig. 9 The structure of the fiber bundle with uniform and stable transmission characteristics.

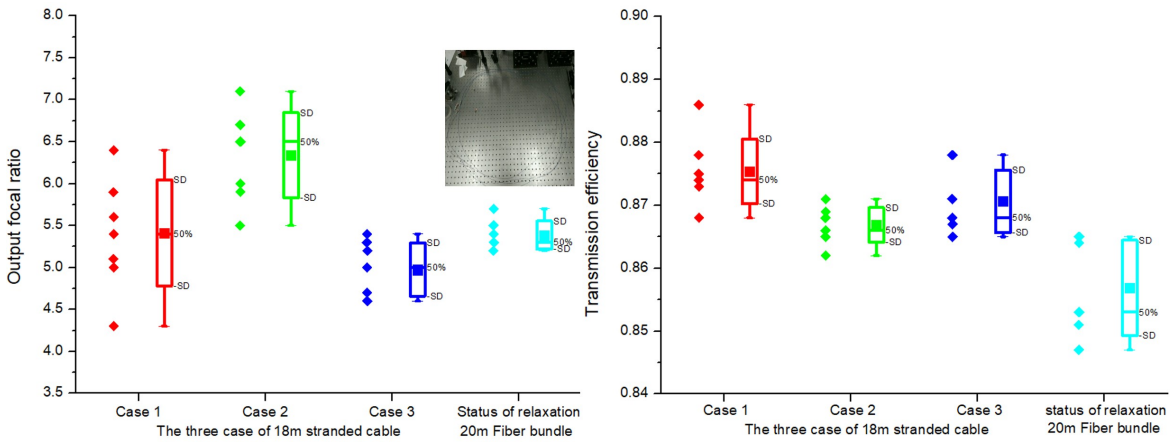


Fig. 10 Transmission characteristics of an 18 m stranded cable and a 20 m fiber bundle. The fiber bundle is in a relaxed state with incident focal ratio $F/8$. (a) Output focal ratio; (b) TE.

bundle decreased significantly. In addition, the maximum difference in OFR increases to 0.9.

For the design of optical cables, the radius of the helix in the cable should be significantly greater than the radius which leads to a significant decreased uniformity in the OFR of the fiber bundle. Murray (2006) suggested that the minimum bending radius of fibers used for astronomy

should be bigger than 200 times the fiber diameter to avoid FRD. The bending radius of a fiber bundle, which can be viewed as a single fiber, also should follow this guideline. The bending radius B of a helix is defined by

$$B = R \left[1 + \left(\frac{P}{4\pi R} \right)^2 \right]. \quad (9)$$

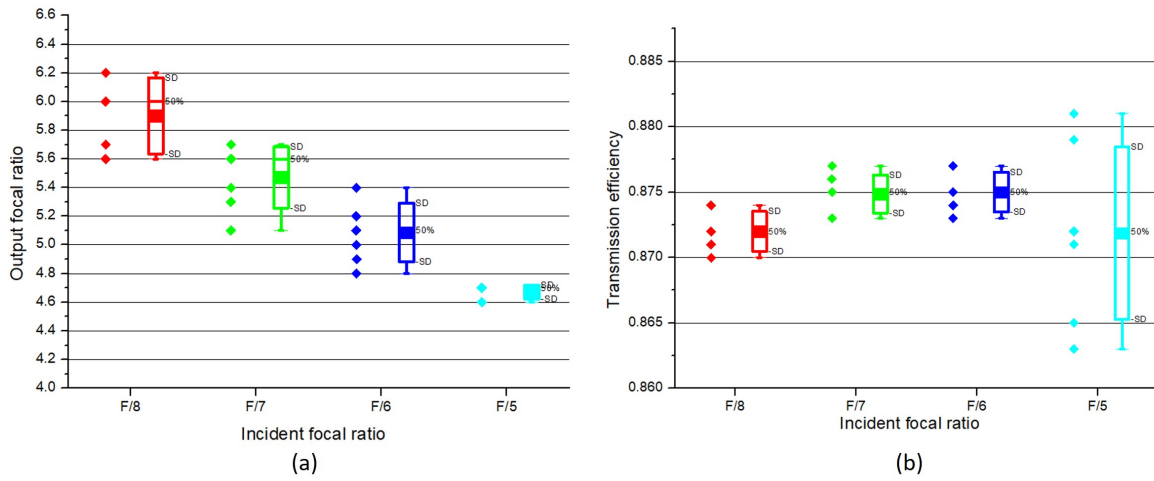


Fig. 11 Transmission characteristics of a 10 m fiber bundle with different incident focal ratios. (a) Output focal ratio; (b) TE.

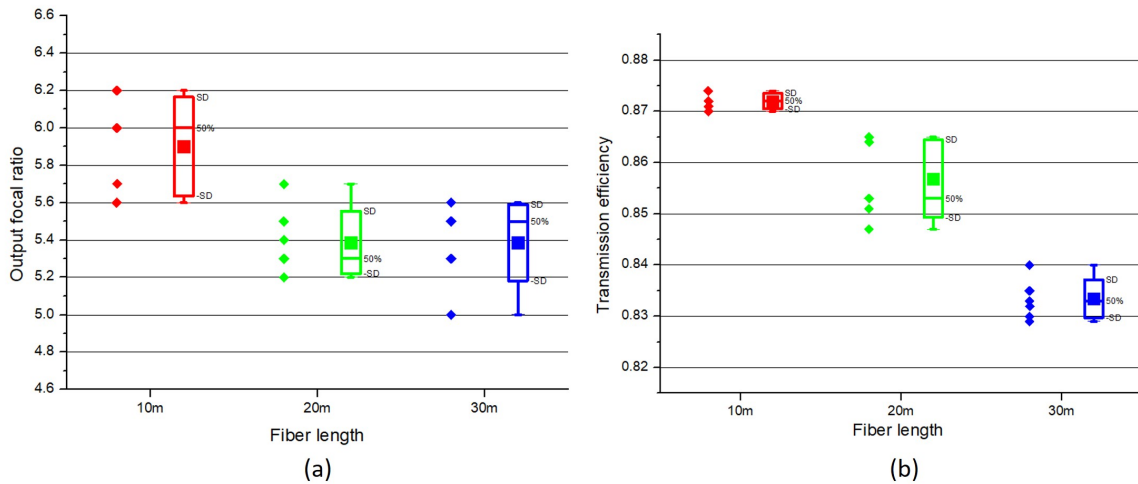


Fig. 12 Transmission characteristics of a fiber bundle with different lengths and incident focal ratio $F/8$. (a) Output focal ratio; (b) TE.



Fig. 13 The fiber bundle with a fixed bending radius at a distance of 1 m from the exit of the optical fiber bundle.

5.5 The FRD with Different Tensions

The tension leads to the deformation of a fiber bundle. When the state of fibers in a bundle changes, the OFR of the fibers also changes. The tension of a fiber bundle is another very important parameter for optical cable design.

The cable structure should keep the fiber bundle in a comfortable state, when the cable is pulled. We tested the transmission characteristics and deformation of the fiber bundle under different tensions. The testing device is shown in Figure 15. After 1 m from the exit end of the optical fiber bundle, the fiber bundle was fixed on the plate and

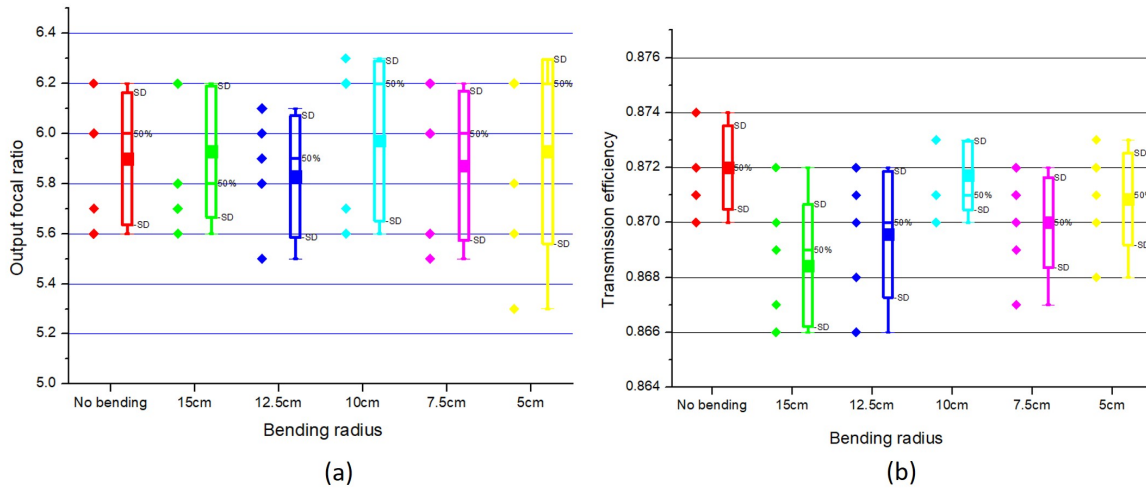


Fig. 14 Transmission characteristics of a fiber bundle with different bending radius and incident focal ratio $F/8$. (a) Output focal ratio; (b) TE.

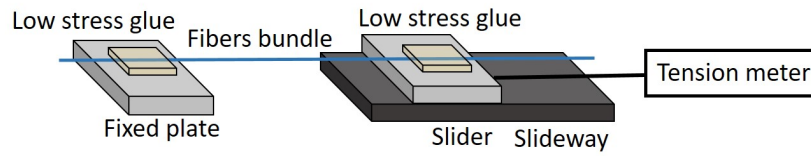


Fig. 15 Bundle deformation with tension.

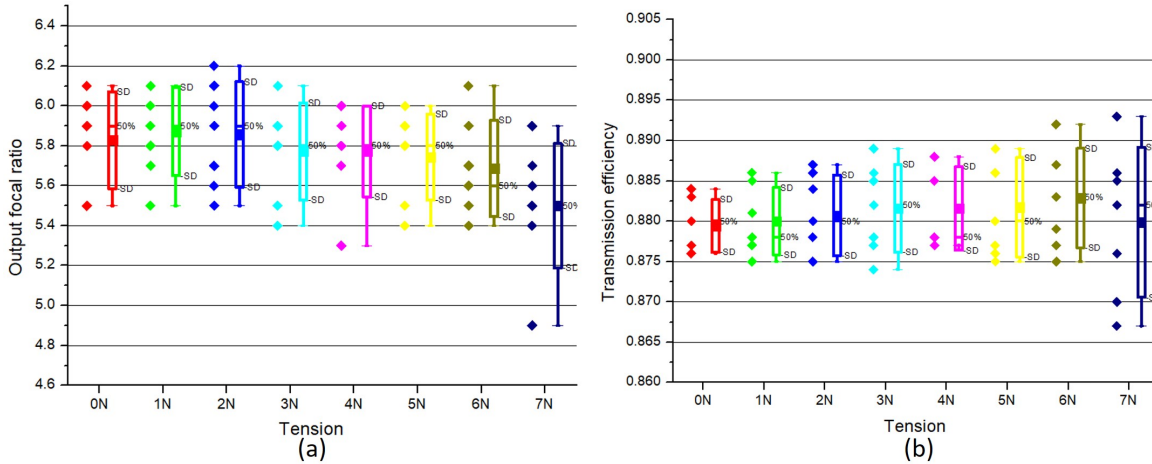


Fig. 16 Transmission characteristics of a fiber bundle with tension from 0 N to 7 N and incident focal ratio $F/8$. (a) Output focal ratio; (b) TE.

slider with low stress glue. The tension changed from 0 N–7 N. The test results for the OFR are shown in Table 7 and plotted in Figure 16(a). The test results for the TE are displayed in Table 8 and plotted in Figure 16(b). When the tension was 6 N, the OFR of fiber 3 dropped significantly, from $F/6.2$ to $F/5.6$. When the tension was 7 N, the OFR of fiber 2 dropped significantly, from $F/5.5$ to $F/4.9$. When the tension was 7 N, the TE of optical fibers 4 and 7 dropped 1%. When the tension was increased to 9 N, the

outer jacket of the fiber bundle was broken. The experimental results demonstrate that we should ensure that the bundle in the cable has a tension of less than 6 N to maintain uniform emitting characteristics of fibers in the cable when they are pulled. Figure 17 shows the bundle deformation with tension. When the cable is pulled, the cable structure should guarantee that the bundle strain is less than 0.035.

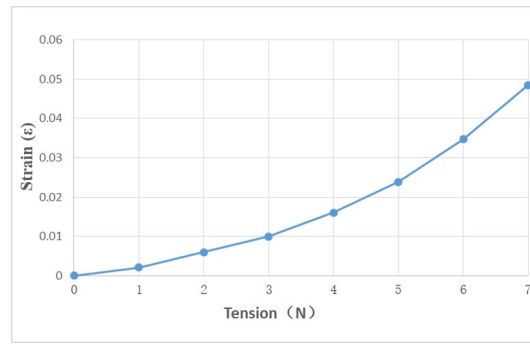


Fig. 17 Bundle deformation with tension.

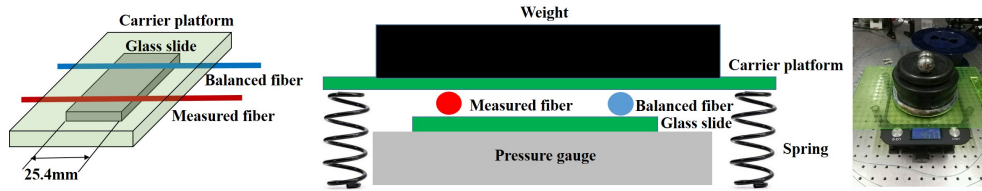


Fig. 18 Device for testing pressure.

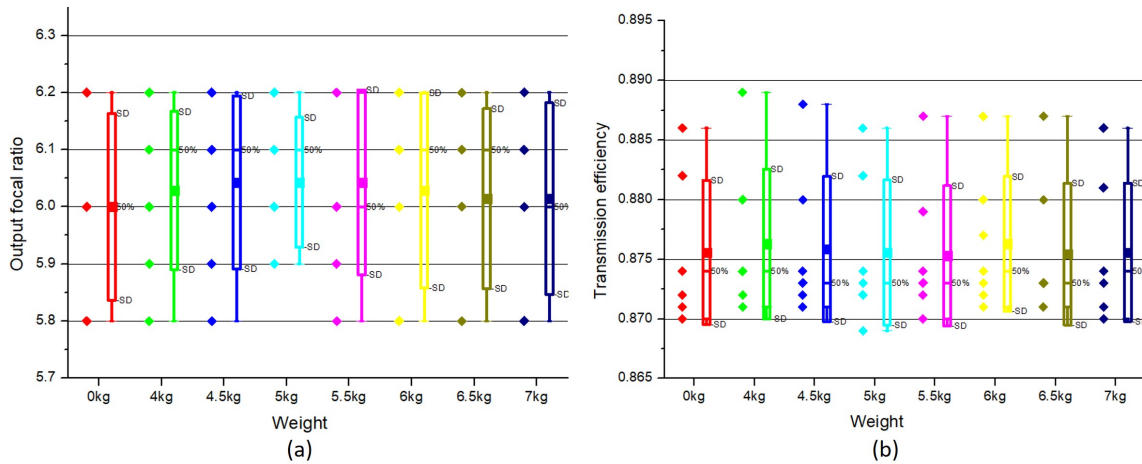


Fig. 19 Transmission characteristics of a fiber bundle with pressure from 4 kg to 7 kg and incident focal ratio $F/8$. (a) Output focal ratio; (b) TE.

5.6 The FRD with Different Pressures

For the FASOT, the IFU will be installed on the strut support of the FASOT telescope. During the operation of the telescope, the telescope pulls the optical cable as it moves while it follows the Sun. The cable state would change with the position of the telescope. As the basic unit, the jacket outside of the fiber bundle should be able to withstand a certain stress from the other fiber bundles and the inner wall of the fiber optic cable. We measured the transmission characteristics of a fiber bundle with different pressures. The testing device is illustrated in Figure 18. We adjusted the pressure by changing the weight from 0 kg to 7 kg. The force point is 1 m away from the exit end of the fiber. The OFR is listed in Table 9 and plotted in Figure 19(a), while

the TE is listed in Table 10 and plotted in Figure 19(b). It is apparent that stress less than 1.38 N mm^{-1} does not aggravate the transmission characteristics of the fiber bundle.

6 SUMMARY

We design and fabricate a fiber bundle as a basic unit of the miniaturized high-density astronomical optical cables utilized in FASOT-IFU. The fibers in the bundle were accurately positioned by UV-curing acrylate. The fiber bundle has uniform transmission characteristics in a relaxed state, especially with an incident focal ratio of $F/5$. The length of the bundle does not affect the uniformity of its emitting characteristics. The jacket formed by the UV-curing acrylate can withstand a certain stress less than 1.38 N mm^{-1} . For the design and wiring of optical cables, the minimum

Table 9 The OFR of a Fiber Bundle with Pressure from 4 kg to 7 kg and Incident Focal Ratio $F/8$

Fiber number	0 kg	4.0 kg	4.5 kg	5.0 kg	5.5 kg	6.0 kg	6.5 kg	7.0 kg
1	6.0	6.1	6.1	6.1	6.2	6.1	6.1	6.1
2	6.2	6.1	6.2	6.1	6.2	6.2	6.1	6.2
3	6.0	6.0	6.0	6.0	6.0	6.0	6.0	6.0
4	6.0	6.1	6.1	6.1	6.0	6.1	6.1	6.0
5	5.8	5.9	5.9	5.9	5.9	5.8	5.8	5.8
6	5.8	5.8	5.8	5.9	5.8	5.8	5.8	5.8
7	6.2	6.2	6.2	6.2	6.2	6.2	6.2	6.2
Average	6.1	6.0	6.0	6.0	6.0	6.0	6.0	6.0
Maximum difference	0.4	0.4	0.4	0.3	0.4	0.4	0.4	0.4

Table 10 The TE of a Fiber Bundle with Pressure from 4 kg to 7 kg and Incident Focal Ratio $F/8$

Fiber number	0 kg	4.0 kg	4.5 kg	5.0 kg	5.5 kg	6.0 kg	6.5 kg	7.0 kg
1	87.1%	87.4%	87.3%	87.3%	87.2%	87.4%	87.3%	87.4%
2	88.2%	88.0%	88.0%	88.2%	87.9%	88.0%	88.0%	88.1%
3	88.6%	88.9%	88.8%	88.6%	88.7%	88.7%	88.7%	88.6%
4	87.4%	87.2%	87.1%	86.9%	87.0%	87.1%	87.1%	87.0%
5	87.2%	87.4%	87.4%	87.4%	87.4%	87.7%	87.3%	87.3%
6	87.4%	87.1%	87.2%	87.2%	87.2%	87.2%	87.1%	87.1%
7	87.0%	87.4%	87.3%	87.3%	87.3%	87.3%	87.3%	87.4%
Average	87.6%	87.6%	87.6%	87.5%	87.6%	87.5%	87.6%	87.6%
Maximum difference	1.8%	1.7%	1.7%	1.7%	1.6%	1.6%	1.6%	1.6%

bending radius should be bigger than 200 times the fiber bundle's outer radius. The fiber bundle can maintain uniform emitting characteristics with a tension of less than 6 N. When the cable is pulled, the cable structure should ensure that the bundle strain is less than 0.035.

Acknowledgements This work was funded by the Joint Research Fund in Astronomy under cooperative agreement between the National Natural Science Foundation of China (NSFC) and the Chinese Academy of Sciences (Grant Nos. U1631239 and U1831115), the NSFC (Grant No. 11603008) and the Fundamental Research Funds for Central Universities to Harbin Engineering University.

References

- Chattopadhyay, S., Joshi, V., Ramaprakash, A. N., et al. 2018, Proc. SPIE, 10706, 107062D
- Cheng, B.-Y. 2016, Design and Manufacture for Optical Fiber and Fiber Optic Cable, 69 (3rd ed; Hangzhou; Zhejiang Univ. Press)
- Chung, H., Ramaprakash, A. N., Omar, A., et al. 2014, Proc. SPIE, 9147, 91470V
- Chung, H., Ramaprakash A. N., Khodade P., et al. 2018, Proc. SPIE, 10702, 107027A
- Cui, X.-Q., Zhao, Y.-H., Chu, Y.-Q., et al. 2012, RAA (Research in Astronomy and Astrophysics), 12, 1197
- Flaugher, B., & Bebek, C. 2014, Proc. SPIE, 9147, 91470S
- Hill, G. J., MacQueen, P. J., Tejada, C., et al. 2004, Proc. SPIE, 5492, 251
- Hill, G. J., Tuttle, S. E., Drory, N., et al. 2014, Proc. SPIE, 9147, 91470Q
- Kelz, A., Jahn, T., Haynes, D., et al. 2014, Proc. SPIE, 9147, 914775
- Lee, H., Chonis, T. S., Hill, G. J., et al. 2010, Proc. SPIE, 7735, 77357H
- Murphy, J. D., Hill, G. J., MacQueen, P. J., et al. 2012, Proc. SPIE, 8446, 84465F
- Murray, G. J. 2006, New Astronomy Reviews, 50, 316
- Murray, G., Tamura, N., Takato, N., et al. 2017, Proc. SPIE, 10401, 104011R
- Qu, Z.-Q. 2011, Proceedings of 6th Solar Polarization, 423
- Qu, Z.-Q., Chang, L., Cheng, X.-M., et al. 2014, Proceedings of 7th Solar Polarization, 263
- Sato, F., Ryan, K., Nagao, Y., et al. 2017, in Proceedings of the 66th IWCS Conference, International Wire & Cable Symposium, 304
- Vattiat, B. L., Lee, H., Chonis, T., et al. 2016, Proc. SPIE, 9908, 99083O
- Yan, Y.-X., Yan, Q., Wang, G., et al. 2018, MNRAS, 476, 4279
- Zhi, L., Qu, Z.-Q., & Yan, X.-L. 2016, Astrophysics and Space Science, 361, 159